



Research Article

A portable smartphone-based colorimetric sensor that utilizes dual amplification for the on-site detection of airborne bacteria

Jisun Ki^{a,b}, Ik Hwan Kwon^c, Jina Lee^{a,d}, Jaewoo Lim^{a,e}, Soojin Jang^{a,d}, Seong Uk Son^{a,d}, Seung Beom Seo^{a,f}, Seo Yeong Oh^a, Taejoon Kang^{a,g}, Juyeon Jung^{a,g}, Kyoung G. Lee^h, Jungho Hwangⁱ, Eun-Kyung Lim^{a,d,g,*}

^a Bionanotechnology Research Center, Korea Research Institute of Bioscience and Biotechnology (KRIBB), Daejeon 34141, Republic of Korea

^b Center for Systems Biology, Massachusetts General Hospital, Harvard Medical School, Boston, MA 02114, USA

^c Safety Measurement Institute, Korea Research Institute of Standards and Science, Daejeon 34113, Republic of Korea

^d Department of Nanobiotechnology, KRIBB School of Biotechnology, University of Science and Technology, 125 Gwahak-ro, Yuseong-gu, Daejeon 34113, Republic of Korea

^e Medical Device Development Center, Osong Medical innovation foundation, 123, Osongsaengmyeong-ro, Chungcheongbuk-do, 28160, Republic of Korea

^f Department of Cogno-Mechatronics Engineering, Pusan National University, 2 Busandaehak-ro 63beon-gil, Geumjeong-gu, Busan 46241, Republic of Korea

^g School of Pharmacy, Sungkyunkwan University, Suwon 16419, Republic of Korea

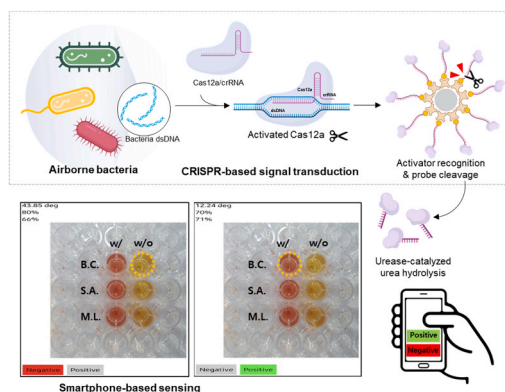
^h Division of Nano-Bio Sensors/Chips Development, National NanoFab Center (NNFC), Daejeon 34141, Republic of Korea

ⁱ Department of Mechanical Engineering, Yonsei University, Seoul 03722, Republic of Korea

HIGHLIGHTS

- In this study, a colorimetry-based bacterial detection platform was designed.
- The platform uses a Cas12a system to amplify signals.
- A urease enzyme induces the color changes.
- A smartphone app that detects colors based on hue saturation value was developed.
- This method can be widely used for public safety as it could prevent epidemics.

GRAPHICAL ABSTRACT



Abbreviations: CRISPR, clustered regularly interspaced short palindromic repeats; Cas12a, CRISPR-associated protein 12a; WHO, World Health Organization; PCR, polymerase chain reaction; ssDNA, single-stranded DNA; Sulfo-SMCC, sulfosuccinimidyl-4-(N-maleimidomethyl)cyclohexane-1-carboxylate; EDTA, ethylenediaminetetraacetic acid; PBS, phosphate-buffered saline; LB, Luria-Bertani; TSB, tryptic soy broth; DEPC, diethylpyrocarbonate; DW, distilled water; crRNA, CRISPR RNA; B.C., *Bacillus cereus*; S.A., *Staphylococcus aureus*; M.L., *Micrococcus luteus*; gDNA, genomic DNA; RGB, red, green, and blue; HSV, hue saturation value; urDNA, urease-modified single-stranded DNA.

* Corresponding author at: Bionanotechnology Research Center, Korea Research Institute of Bioscience and Biotechnology (KRIBB), Daejeon 34141, Republic of Korea.

E-mail address: eklim1112@kribb.re.kr (E.-K. Lim).

<https://doi.org/10.1016/j.jhazmat.2023.132398>

Received 18 June 2023; Received in revised form 22 August 2023; Accepted 23 August 2023

Available online 25 August 2023

0304-3894/© 2023 The Authors. Published by Elsevier B.V. This is an open access article under the CC BY-NC-ND license (<http://creativecommons.org/licenses/by-nc-nd/4.0/>).

ARTICLE INFO

Editor: Shaily Mahendra

Keywords:

Colorimetry
Pathogen
Mobile
Bacterial detection
Point-of-care sensing

ABSTRACT

Over the past few years, infections caused by airborne pathogens have spread worldwide, infecting several people and becoming an increasingly severe threat to public health. Therefore, there is an urgent need for developing airborne pathogen monitoring technology for use in confined environments to enable epidemic prevention. In this study, we designed a colorimetry-based bacterial detection platform that uses a clustered regularly interspaced short palindromic repeat-associated protein 12a system to amplify signals and a urease enzyme to induce color changes. Furthermore, we have developed a smartphone application that can distinguish colors under different illumination conditions based on the HSV model and detect three types of disease-causing bacteria. Even synthetic oligomers of a few picomoles of concentration and genomic DNA of airborne bacteria smaller than several nanograms can be detected with the naked eye and using color analysis systems. Furthermore, in the air capture model system, the bacterial sample generated approximately a 2-fold signal difference compared with that in the control group. This colorimetric detection method can be widely applied for public safety because it is easy to use and does not require complex equipment.

1. Introduction

Airborne microorganisms such as viruses, fungi, and bacteria can pose severe risks to human health, causing numerous social burdens. As of June 2021, severe acute respiratory syndrome coronavirus 2 had infected more than 178 million individuals and caused 3.8 million deaths, as reported by the World Health Organization (WHO) [1,16]. Furthermore, microorganisms, particularly bacteria, are ubiquitous and commonly encountered by humans. Additionally, infections caused by these microbes are responsible for the frequent outbreaks of airborne diseases. According to WHO reports, approximately 10 million people are affected by illnesses caused by bacterial infections, accounting for 20% of annual deaths globally [27]. Therefore, efforts to develop early and rapid diagnosis methods aim to reduce pathogen transmission rates

and prevent pathogen-related illnesses [19].

Several techniques have been extensively used, including culture, immunoassays, and polymerase chain reaction (PCR)-based systems. However, culture-based methods have the disadvantages of being prone to contamination, being time- and resource-intensive, and relying on phenotypic biochemical characterization [4]. Although immunoassay and PCR methods provide high sensitivity and specificity, they require expensive reagents and analytical equipment [26]. Specifically, the electrochemical technique is highly accurate; however, its uniformity is poor owing to the non-commercial electrodes [7]. As it is difficult to quickly detect and immediately identify airborne bacteria, a rapid, simple, and inexpensive method for bacterial detection is urgently required.

Optical biosensors have unique advantages, including portability,

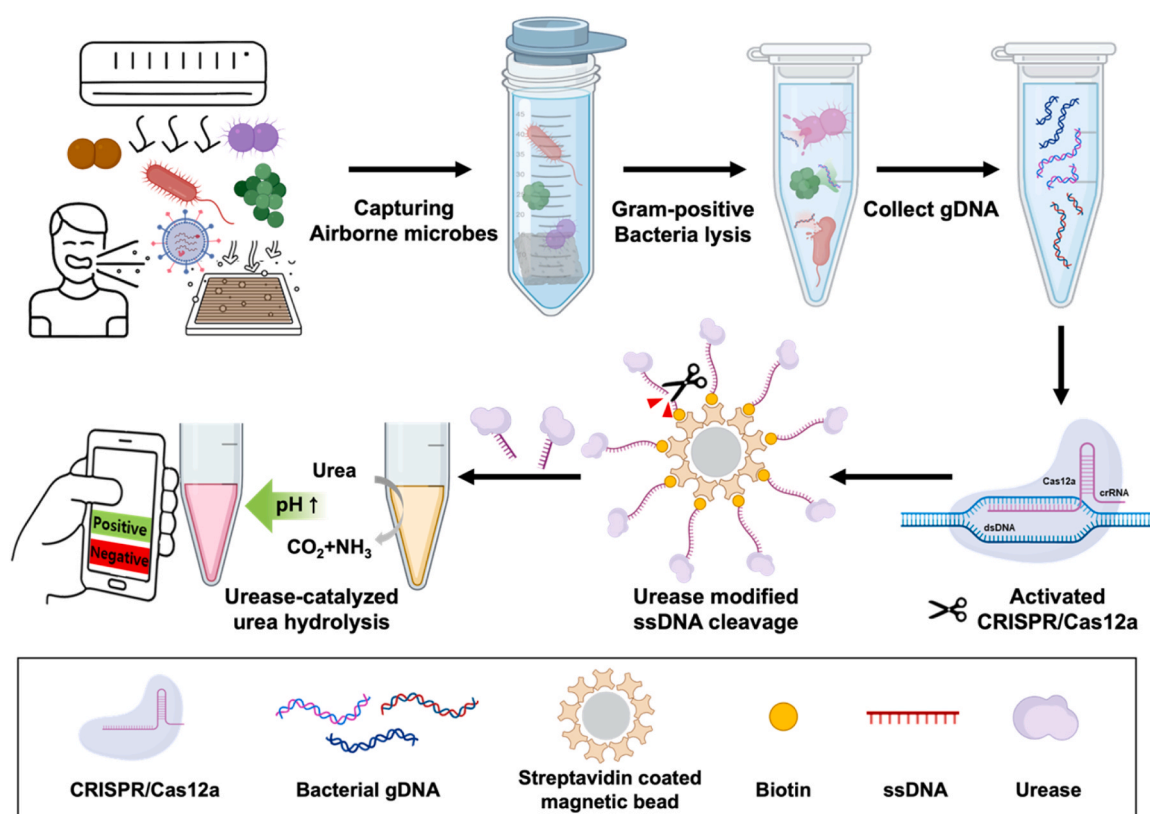


Fig. 1. Schematic illustration of colorimetric bacteria detection based on dual enzyme amplification using Cas12a and urease. Gram-positive bacteria are lysed to release genes, among various biomarkers, including airborne bacteria and viruses. CRISPR/Cas12a is activated by recognizing a specific genomic DNA sequence (gDNA) and exhibits collateral cleavage properties. Activated CRISPR/Cas12a cleaves urease-conjugated ssDNA immobilized on magnetic beads. The released urease increases the pH and changes the color of the sample in the presence of phenol red, from yellow to magenta. The custom-designed smartphone application converts the optical output into the color space mode and reports the disease status.

low cost, and ease of use. Among these biosensors, the colorimetric assay is suitable for on-site detection because the results can be read directly with the unaided eye [23]. In addition, when a colorimetric analysis system is combined with a smartphone, it can be used as a proof-of-concept system whose output can be analyzed immediately without separate analysis equipment [29,30]. Colorimetric techniques that have recently been developed use changes in the shape and size of plasmonic nanoparticles, such as gold nanoparticles, for detection. Additionally, some methods use color changes resulting from pH and metabolite production using enzymes [18]. However, plasmonic nanoparticles have a disadvantage in that signal reproducibility is irregular because the synthesis process for uniformity is complicated, and aggregation easily occurs under unfavorable pH and salinity conditions [17,24,25,28]. Therefore, we present a method for visually detecting bacteria using enzyme-based colorimetric changes and a smartphone application (app) for an instrument-free point-of-care system.

We devised a method wherein a clustered regularly interspaced short palindromic repeats (CRISPR)-associated protein 12a (Cas12a) system recognizes a specific sequence of DNA in bacteria and induces a colorimetric change by excising urease-bound single-stranded DNA (ssDNA; Fig. 1). The urease released from the magnetic beads changes the pH of the solution. Furthermore, the phenol red solution induces a color change from yellow to magenta. Numerous bacteria are widely distributed in the air and are reported to be harmful to humans; thus, they were used as experimental models. This study is valuable because our proposed method can easily detect bacteria using a smartphone without requiring expensive equipment, skilled researchers, or gene amplification processes. Therefore, this analytical technology can help monitor airborne bacteria in public places and offices and aid in rapidly developing countermeasures.

2. Experimental

2.1. Materials and Instruments

Modified DNA oligonucleotides were purchased from Integrated DNA Technologies (Coralville, IA, USA) and Bioneer (Daejeon, Republic of Korea). The oligonucleotide sequence information of the probes used in this study is listed in Table S1. Sulfo-succinimidyl-4-(N-maleimidomethyl)cyclohexane-1-carboxylate (Sulfo-SMCC), ethylenediaminetetraacetic acid (EDTA), Tween® 20, urea, phenol red, urease from *Canavalia ensiformis* (Jack bean), and sodium chloride were obtained from Sigma-Aldrich (St. Louis, MO, USA). Dynabeads™ M-270 streptavidin—streptavidin-coated superparamagnetic beads—were obtained from Thermo Fisher Scientific (Waltham, MA, USA). Dulbecco's phosphate-buffered saline (PBS; Cat. No. LB 001-02) was purchased from Welgene (Gyeongsan, Republic of Korea). EnGen® Lba Cas12a (Cpf1) was purchased from New England BioLabs (Ipswich, MA, USA). Moreover, 1 M Tris-HCl (pH 7.2) was purchased from Biosesang (Seongnam, Republic of Korea). All other chemicals and reagents were of analytical grade. A G-spin Genomic DNA Extraction kit (for bacteria) was purchased from Intron (Seongnam, Republic of Korea). A Synergy H1 hybrid multi-mode microplate reader and Cytation hybrid multi-mode reader (Agilent Technologies, Winooski, VT, USA) were used for measuring fluorescence. Luria-Bertani (LB) broth was obtained from Condalab (Madrid, Spain), tryptic soy broth (TSB) was purchased from BD Biosciences (San Jose, CA, USA), and agar plates were obtained from Promega (Madison, WI, USA).

2.2. Preparation of urease-modified single-stranded DNA (urDNA)

As described previously, urDNA was synthesized by conjugating urease and ssDNA [21]. First, amine and biotin modifications to the 5'- and 3'- termini of ssDNA solution (100 μ M) in diethylpyrocarbonate (DEPC) water and Sulfo-SMCC solution (6.4 mM) in water were prepared. A final volume of 100 μ L of PBS buffer was adjusted with 10 μ L of

ssDNA (1 nmol) and 7 μ L of Sulfo-SMCC (45 nmol). Subsequently, they were reacted at 25 °C for 1 h. Thereafter, this mixture was passed through a centrifugal filter with a molecular weight cut-off of 3 kDa (Merck Millipore, Billerica, MA, USA) to remove excess Sulfo-SMCC and obtained maleimide-activated DNAs. Next, 10 μ M of DNAs resuspended in 100 μ L of PBS and urease (1.5 mg) dispersed in 400 μ L of PBS were mixed in an acidic buffer (pH 6.5) at 25 °C overnight to conjugate with the maleimide-DNAs and the thiol of urease. The mixture was filtered through a 100-kDa cut-off centrifugal column (Merck Millipore) and then resuspended in 100 μ L of PBS to obtain a concentration of 10 μ M urDNA.

2.3. Fabrication of magnetic beads immobilized with urDNA (MB@urDNA)

First, 300 μ g of magnetic beads were washed twice using 500 μ L of binding and washing buffer (B/W buffer; 5QWDF mM Tris-HCl, 0.5 mM EDTA, 1 M NaCl, and 0.05% Tween 20; pH 7.5). Next, after resuspending in 500 μ L of B/W buffer, 100 pmol of urDNA was added and incubated for 2 h with gentle rotation at 1 rpm. Subsequently, MB@urDNA was magnetically separated and washed thrice with 500 μ L B/W buffer. Thereafter, it was dispersed in 30 μ L of B/W buffer, and 10 mg/mL of MB@urDNA was obtained.

2.4. Collateral DNase activity using Cas12a

CRISPR/Cas12a solution was prepared by mixing equal volumes of 2 μ M *Lachnospiraceae bacterium* Cas12a and 1 μ M CRISPR RNA (crRNA) at 37 °C for 1 h. Solutions of 50 μ L containing 10 μ L of various concentrations of dsDNA were prepared to confirm the collateral DNase activity of Cas12a based on fluorescence. Thereafter, 2 μ L of reporter probe FAM-ssDNA-BHQ2 (50 μ M) was mixed with 10 μ L of Cas12a/crRNA (0.5 μ M), 5 μ L of 10 \times NEBuffer 2.1, and 23 μ L of DEPC-treated water. After dsDNA treatment, the fluorescence intensity of the solution was measured using a hybrid-multi-mode microplate reader and monitored at an excitation and emission wavelength of 480 and 520 nm, respectively. In addition, for the colorimetric assay using MB@urDNA, the reaction solution was prepared as a 50- μ L solution containing 5 μ L of various concentrations of the dsDNA, 30 μ L of MB@urDNA (10 mg/mL), 10 μ L of Cas12a/crRNA (0.5 μ M), and 5 μ L of 10 \times NEBuffer 2.1. Furthermore, this reactant was incubated at 37 °C for 30 min. After separating impurities with a magnet, 40 μ L of supernatant was transferred into a 96-well microplate well. Subsequently, 10 μ L of PBS, 130 μ L of urea substrate solution (2 M NaCl, 60 mM MgCl₂, 50 mM urea, and 1 mM HCl), and 0.04% phenol red were added.

2.5. Preparation of bacterial culture

All bacteria [*Bacillus cereus* (B.C.), *Staphylococcus aureus* (S.A.), and *Micrococcus luteus* (M.L.)] used in this study were provided by the Korean Collection for Type Cultures. LB and TSB solutions were prepared by adding 5 g of LB and 6 g of TSB in a bottle sterilized by autoclaving and 200 mL of distilled water (DW). LB agar plates were prepared by adding 12.5 g of LB and 7.5 g of agar with 500 mL of DW. The bacterial culture was prepared by mixing 15 mL LB broth and bacteria in a 50-mL conical tube and incubating overnight in a shaking incubator at 37 °C and 180 rpm. Bacterial genomic DNA (gDNA) extraction was performed using the G-spin Genomic DNA Extraction kit (Cat. No. 17121; iNtRON Biotechnology, Seongnam, Republic of Korea) following the manufacturer's instructions. In addition, bacteria were collected from airborne aerosols using an electrostatic sampler at room temperature for 2 h [11,12]. After culturing the collected samples, the bacterial species in the samples were identified using matrix-assisted laser desorption ionization time-of-flight mass spectrometry analysis.

2.6. Bacterial gDNA sensing

A 5 μL drop of *S. Aureus* solution with a concentration of 1×10^9 cells/mL was placed on the 0.5×0.5 cm nanosubstrate with an urchin-like nanostructure and incubated for 30 min in a humid environment. After washing the nanostructure absorbed *S. Aureus* with PBS three times, the substrate was immersed in a 30 μL PBS solution and heated at 95°C for 10 min to release the gDNA from *S. Aureus*. The reaction solution, consisting of 30 μL of MB@urDNA (10 mg/mL), 15 μL of Cas12a/crRNA (2 μM), and 5 μL of $10 \times$ NEBuffer 2.1, was added to the solution containing the released gDNA. The reaction was then incubated at 37°C for 30 min, during which the urDNA oligomers on the MB surface were cleaved by Cas12a/crRNA. After separating the MB, the supernatant containing urease dissociated from MB was transferred into one well of a 96-well microplate. Subsequently, 130 μL of urea substrate solution, 10 μL of PBS, and 0.04% phenol red were added, and the absorption and hue values of the solution were measured.

2.7. Smartphone app development for colorimetric analysis of bacterial detection

The bacterial activation diagnostic app was developed using MIT App Inventor, a visual programming environment that allows functional app programming for smartphones and tablets [20]. A Samsung Galaxy S10 5 G model was used to obtain the image, and the specifications of the camera used here are 12 MP, $f/2.4$, 52 mm (telephoto), $1/3.6''$, 1.0 μm , AF, OIS, and $2 \times$ optical zoom. The software algorithm created using the program inventor, and more detailed information is in the supporting information. Urease changes the absorbance of the media, which is a strategy of diagnosing bacteria based on color formation.

3. Results and discussion

3.1. DNase activity of Cas12a guided by crRNA

For the design of bacterial detection proof-of-concept, we chose three types of gram-positive bacteria, namely, B.C., S.A., and M.L., which are widely distributed in air and food and are harmful to humans; therefore, they were used as experimental models [13,21,5,6,8]. To apply the CRISPR/Cas12a detection system, a crRNA capable of recognizing bacterial gDNA containing a 5'-terminal TTTV protospacer adjacent motif sequence is required (Table S1). In this study, we selected crRNAs showing low G-quadruplex formation and low overlapping efficiency using the CRISPRscan program (<http://CRISPRscan.org>). After complementary hybridization between bacterial gDNA and crRNA, CRISPR/Cas12a is activated and cleaves nearby ssDNA. Therefore, we first evaluated the DNase activity of CRISPR/Cas12a in the presence of bacterial gDNA for crRNA sequence conformity. For the activation assay of Cas12a, FAM-modified ssDNA was immobilized on magnetic beads. When bacterial gDNA is present, activated Cas12a cleaves the ssDNA, increasing the fluorescence signal (Fig. 2a). In Fig. 2b, the fluorescence graphs show that the signal increases approximately 4.0-, 4.5-, and 3.8-fold in the presence of B.C., S.A., and M.A., respectively, compared with that in the off-target condition. The absolute intensity of the fluorescence signal differs slightly depending on the type of bacteria; however, the increase pattern and rate are similar for the three conditions. Moreover, this result indicated that the fluorescence signal increased 3.7-, 4.3-, and 3.2-fold for B.C., S.A., and M.A., respectively, compared with that for the control group, even under the 60-min reaction condition. Moreover, we confirmed that the crRNA we designed detected gDNA extracted from bacteria (Fig. 2c). As the results of Fig. 2b proved that the reaction time of 60 min was sufficient, the reaction between CRISPR/Cas12a and gDNA was observed for 1 h. The fluorescence intensities of B.C., S.A., and M.L. were 2.2-, 2.0-, and 1.8-fold higher, respectively, than that in the condition where gDNA was absent. Finally,

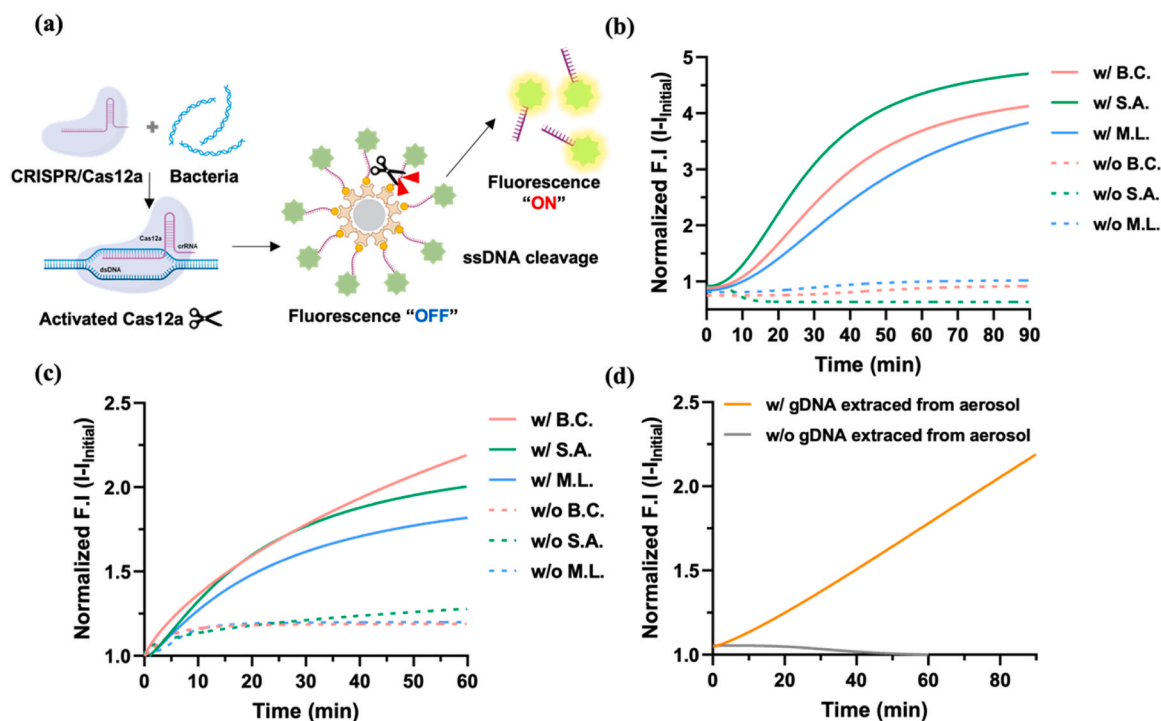


Fig. 2. (a) Illustration of fluorescence-based CRISPR/Cas12a assay validation. Fluorescence kinetics measurements using synthetic (b) dsDNA oligomer and (c) the genomic DNA (gDNA) extracted from cultured bacteria. (d) The fluorescence signal for detection of bacterial gDNA extracted from an airborne aerosol. (*Bacillus cereus*: B.C., *Staphylococcus aureus*: S.A., and *Micrococcus luteus*: M.L.). [illustration created using BioRender.com].

fluorescence kinetics were confirmed using bacterial genetic samples collected from the air (Fig. 2d).

When reacting for 60 and 90 min, the fluorescence signal increased 1.7- and 2.25-fold, respectively, compared with that in the control group. Collectively, we demonstrated that the designed crRNA recognizes the actual bacterial sequence and activates CRISPR/Cas12a.

3.2. Establishment of a smartphone-based color analysis app

We presented a colorimetric detection method using urease to accurately determine numerical values (Fig. 3). When urease is present in a sample containing urea and phenol red, urease hydrolyzes urea and increases the pH, changing the color of the solution from yellow to magenta. When reacted for 5 min, the color difference can be visually recognized at a urease concentration of 3.9 $\mu\text{g/mL}$ or more (Fig. 3a). The color of the solution at a concentration lower than 3.9 $\mu\text{g/mL}$ was visually distinct when reacted for 30 min (Fig. S1). The change in visible

color is associated with the difference in the absorption spectrum. Each condition with different urease concentrations was distinguished by the absorbance spectrum. It was shown that the peak at 430 nm decreased and that at 560 nm increased as the urease concentration increased (Fig. 3b). However, absorption spectrum analysis has a disadvantage in that the absorbance intensity easily changes when the concentration of phenol red is slightly lower or when the volume of the entire solution is slightly altered. Analyzing the absorbance ratio of 460 and 560 nm is a strategy to reduce the experimental error (Fig. 3c).

Furthermore, analyzing the 460 and 560 nm absorbance ratios showed results consistent with the spectral analysis. Absorption-based assays distinguish even low concentrations of urease, therefore we converted the spectrum to color to be applied to smartphones. Because a smartphone camera typically acquires a color image from three primary color arrays: red, green, and blue (RGB), we first converted the spectral data to RGB color values using the Commission Internationale de l'Éclairage 1931 color model (Fig. 3d and S2) [3]. As the 430-nm and

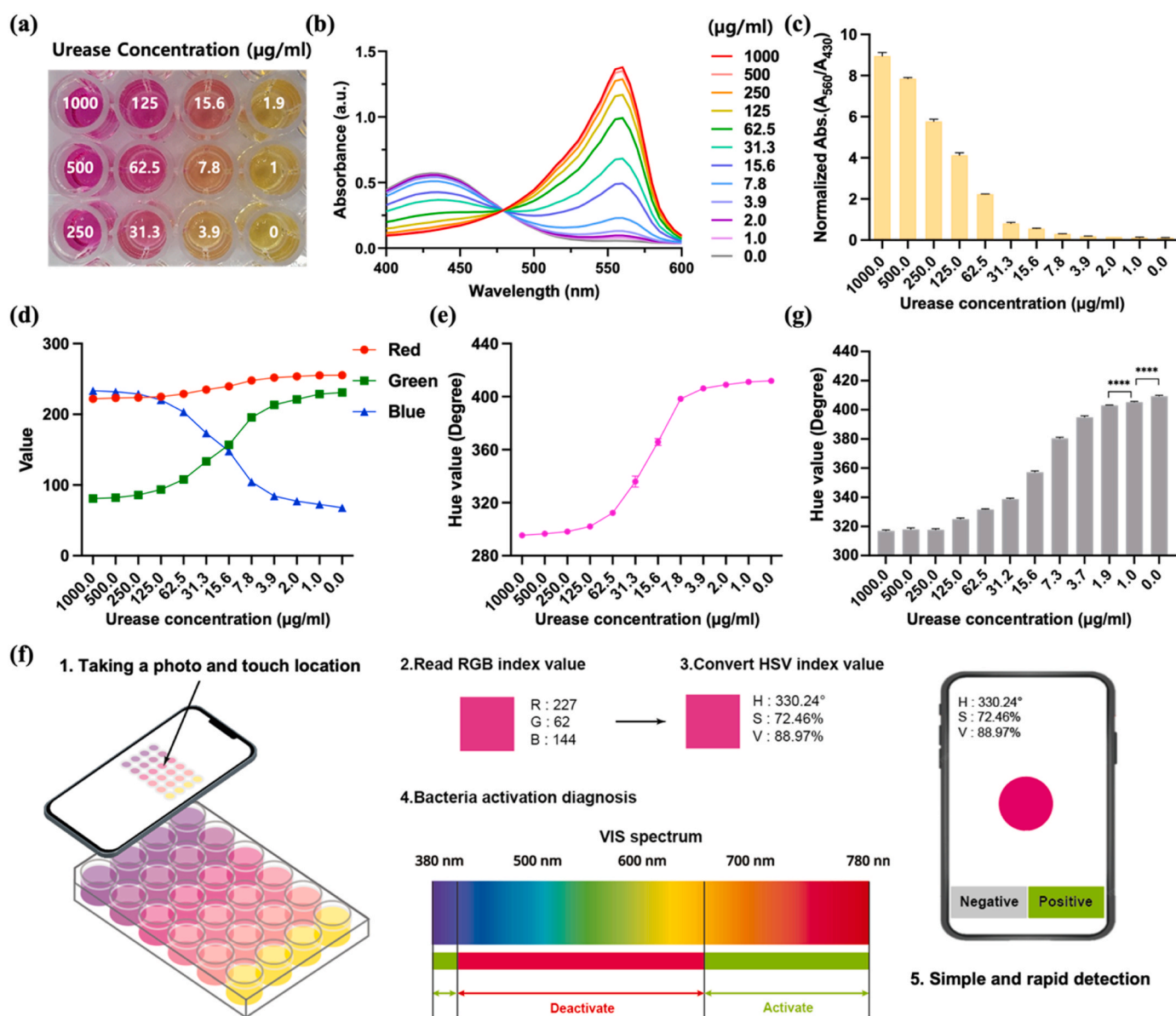


Fig. 3. Analysis of color and development of color recognition app. (a) Photography according to various urease concentrations (0–1000 $\mu\text{g/mL}$) after 5 min reaction. (b) Absorbance graph and (c) normalized absorption values at 560 nm versus 430 nm of the urease concentration. (d) Graph of linear red, green, and blue (RGB) color values converted based on the absorbance spectrum. (e) Graph of the hue values converted the RGB color values. (f) An illustration of the application that detects biomaterials by transforming the color values of the reaction products based on the HSV model. (g) Graph of the hue values measured using the application.

560-nm absorbance spectra of the substrate solution changed with the concentration of urease, the color change of the media was more affected by green and blue than by red. Recently, a study on color analysis using a color indicator including phenol red and a study on diagnosis using changes in a specific color gamut of RGB have been reported [22]. However, comparative studies using specific prime colors among RGB values may yield inaccurate color detection results. To overcome this barrier, we used a color-diagnosis technique using the hue saturation value (HSV) scale (Fig. S3) [14]. Theoretical hue value graphs extracted from the absorption spectra also demonstrate that different concentrations of urease can be distinguished (Fig. 3e). Moreover, the hue-based color analysis method allows for a more intuitive interpretation of RGB. Therefore, we sought to analyze the color by converting RGB to the HSV scale using the CIE color model represented as Equation S1–3. Table S2 shows the converted RGB and HSV from the absorption spectra in which various concentrations of urease were reacted for 5 min. We set the hue value from 300° to 395° (35°) as a positive number using the hue value data, and based on this, we designed an app that determines the disease-causing pathogen by color on a smartphone (Fig. 3f). In Fig. S4, the images demonstrate the functionality of our customized App., which is based on the mentioned algorithms, operating on an actual smartphone. The result of the solution measured using the custom-designed smartphone app was consistent with the absorbance graph and the theoretical hue result value (Fig. 3g). Furthermore, by utilizing the color analysis app based on the HSV model, the measurement values remain unchanged regardless of the brightness and darkness of the measurement background or the presence or absence of light (Fig. S5 and Table S3). Additionally, Fig. S6 shows that there is no difference in the measured hue values when taking photos of the experimental solution at various camera angles and distances. In conclusion, our platform consistently generated statistically identical intensity values, irrespective of various environmental conditions, camera positions, and angles.

3.3. Smartphone-Based Colorimetric Sensing

Next, we studied the detection of bacteria using magnetic beads immobilized with urDNA (Fig. 4). Activated CRISPR/Cas12a cleaves urDNA in the presence of bacterial genes, and the released urease changes the color of the solution (Fig. 4a). A previous study described an optimization experiment for this process [9]. This paper presents the optimal concentrations and incubation time of MB and urDNA for effective color change analysis. The varied color is converted to the hue value by the smartphone app, and we confirmed the presence of bacteria using these data. The absorbance graph shows that the 560-nm intensity when the bacterial target oligomer is present is 3.00-, 4.57-, and 4.88-fold higher for B.C., S.A., and M.L., respectively, then that for the control group (Fig. 4b). Moreover, when bacterial gDNA is present, the 560 and 430 nm ratio shows consistent results (Fig. 4c). The hue values of B.C., S.A., and M.L., analyzed using the smartphone app, are 11.43°, 8.57°, and 12.34°, respectively, and the unwrapped values are 371.43°, 368.57°, and 372.34°, respectively (Fig. 4d). The software algorithm for the smartphone app is presented in Fig. S7. On the smartphone screen, positive and negative are distinguished according to the measured hue value. The cell phone screen image displays a positive sign when bacteria are present and a negative sign when bacteria are absent (Fig. S8).

3.4. Evaluation of actual bacterial detectability using an aerosol bacterial capture model

Subsequently, we evaluated the dual-enzymatic colorimetric assay using various concentrations and types of gene targets and an airborne bacterial capture model (Fig. 5). As shown in Fig. 5a, the response signal decreased as the synthetic bacterial dsDNA concentration increased from 0 M to 50 nM. An image of the reaction solution shows that the color changed from scarlet to yellow as the bacterial gene expression decreased (Fig. 5ai). The absorbance graph for each type of bacteria also

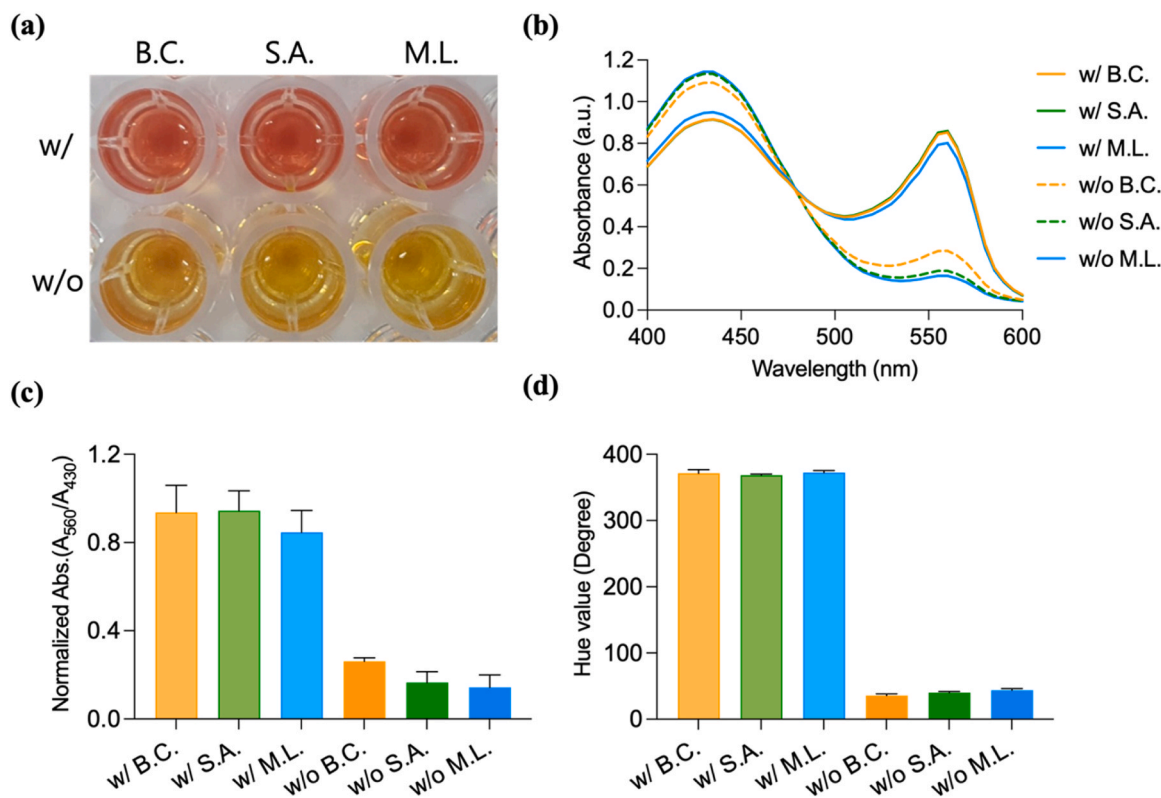


Fig. 4. (a) Photograph of the substrate solution according to the presence or absence of synthesized dsDNA oligomers (250 fmol) and (b) corresponding absorbance graph. B.C., S.A., and M.L. represent *Bacillus cereus*, *Staphylococcus aureus*, and *Micrococcus luteus*, respectively. (c) Graph of the ratio values at 430 nm and 560 nm. (d) Graph of the hue value obtained using a custom-designed App.

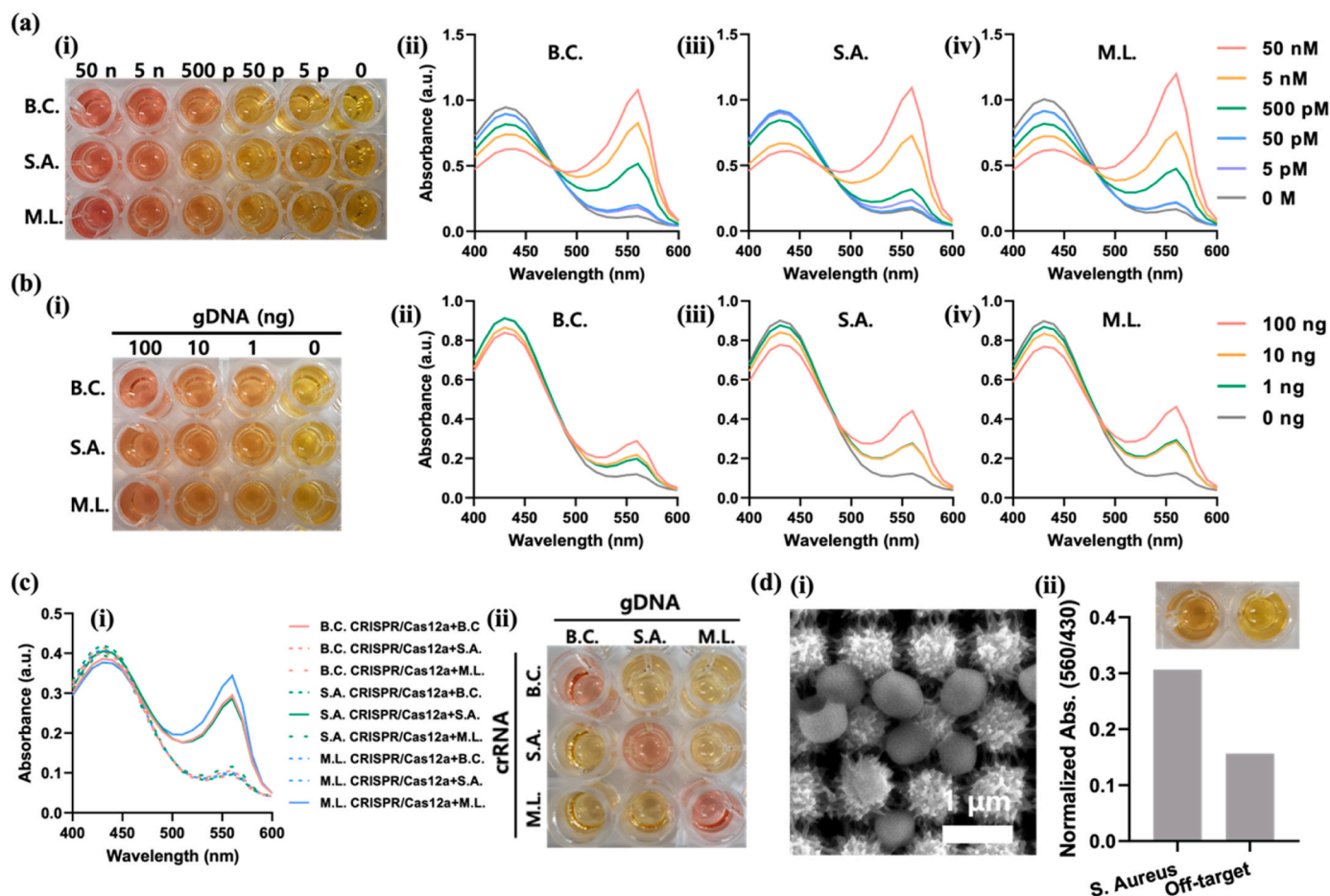


Fig. 5. (a) Sensitivity of the dual-enzymatic colorimetric assay using CRISPR/Cas12a and urease (i) Images of the proposed colorimetric analysis method for detecting various concentrations (0–50 nM) of *Bacillus cereus*, *Staphylococcus aureus*, and *Micrococcus luteus* (referred to as B.C., S.A., and M.L., respectively) and (ii–iv) corresponding absorbance graphs. (b) Validation of gDNA detection assay (i) Corresponding images and (ii–iv) absorbance graph for detection of various concentration of gDNA of B.C., S.A., and M.L., respectively) (c) Absorbance graph (left) and corresponding images (right) of the selectivity using 3-type genomic DNA extracted from cultured bacteria. (d) (i) Scanning electron microscopy image of *Staphylococcus aureus* collected on the substrate. (ii) Absorbance ratio graph at 560 and 430 nm and presence or absence of aerosol bacteria.

showed that the intensity at 560 nm decreased, and the intensity at 430 nm increased according to the concentration (Fig. 5 aii–iv). Although the reactivity is slightly different depending on the type of bacteria, the proposed assay could detect 5 pM genes of all types of bacteria. The absorbance intensities at 560 nm for 5 pM of B.C., S.A., and M.L. were 1.58-, 1.42-, and 1.33-fold higher, respectively, than those for 0 M. The feasibility of practical application was confirmed using gDNA extracted from actual bacteria rather than the synthesized oligomers (Fig. 5b). A color change could be observed with the naked eye in solutions diluted 10- and 100-fold at 100 ng (Fig. 5bi). It was confirmed that the reactivity was slightly different depending on the type of bacteria; however, all of them showed different colorations and absorbance spectra up to 1 ng. The absorbance intensities at 560 nm for 1 ng of B.C., S.A., and M.L. were 1.66-, 2.25-, and 2.34-fold higher, respectively, than those for 0 ng (Fig. 5bii–iv). Fig. 5c shows the cross-reactivity of the three types of bacteria used to evaluate the selectivity of this system. The color and graph changed only for conditions that matched without reacting to conditions inconsistent with each crRNA. Under the condition that the target gene and CRISPR/Cas12a are matched, the maximum absorbance intensities of B.C., S.A., and M.L. were 3.14, 2.99, and 3.37, respectively. The images in Fig. S9 represented the actual smartphone App. results for this experiment. To verify the performance of our sensor, we detected and compared the aerosol bacterial species in the collected sample were identified using matrix-assisted laser desorption/ionization time-of-flight (MALDI-TOF) analysis, one of the

gold standard methods used for the accurate identification of microorganisms such as bacteria [15]. To do this, collected sample from the air were cultured and identified the bacterial species using MALDI-TOF analysis. Therefore, this MALDI-TOF analysis requires takes at least 5 days from culture to analysis. As shown in Figs. S10, 3-species of bacteria, S.A., B. C., and M. L., were mainly confirmed. Furthermore, we introduced hierarchical gold nanostructures to establish models for capturing bacteria in the air and water (Fig. S11) [10–12]. As S.A. causes purulent inflammation and food poisoning, has diverse routes of infection, and is classified as harmful bacteria, S.A. was used as an experimental model. First, as a bacterial capture model, bacteria were adsorbed to alloy nanostructures such as sea urchins, and the scanning electron microscope image shows that bacteria were adsorbed on the nanostructure surface (Fig. 5di). Thereafter, the bacteria-adsorbed nanostructures were heated at 95 °C for 10 min to detect eluting bacterial genes. The absorbance graph shows that the absorbance ratio values of 560 and 430 nm for conditions with and without bacteria were 0.16 and 0.31, respectively (Fig. 5dii). Therefore, we confirmed that the proposed dual enzyme amplification assay could detect bacteria in aerosols using a bacterial adsorption model.

4. Conclusions

In summary, we developed an instrument-free bacterial sensing platform based on urease and crRNA/Cas12a. CRISPR/Cas12a enabled

low-concentration gene detection. Furthermore, multiplexing was possible only by changing the crRNA sequence. In addition, the rapid hydrolysis reaction of urease and the marked color change of phenol red because of pH were suitable for visual observation. This visual sensing platform generates spectral changes at 430 nm and 560 nm, which can be observed with the naked eye. To analyze the color changes accurately and conveniently, we converted these changes using the HSV model, enabling color discrimination under various illuminations conditions. The color recognition smartphone app was developed to distinguish between positive and negative results, making the analysis of color changes precise and user-friendly. This convenient and immediate detection system can be widely applied to diagnose infectious bacteria in air to ensure public safety.

CRedit authorship contribution statement

Jisun Ki: Conceptualization, Methodology, Software, Formal analysis, Investigation, Writing – original draft. **Ik Hwan Kwon:** Methodology, Software, Formal analysis, Investigation. **Jina Lee:** Methodology, Formal analysis. **Jaewoo Lim:** Methodology, Formal analysis. **Soojin Jang:** Formal analysis, Investigation, Visualization. **Seong Uk Son:** Formal analysis, Investigation, Data curation. **Seung Beom Seo:** Formal analysis, Investigation, Data curation. **Seo Yeong Oh:** Formal analysis, Investigation, Data curation. **Taejoon Kang:** Formal analysis, Investigation, Funding acquisition. **Juyeon Jung:** Formal analysis, Investigation, Funding acquisition. **Kyoung G. Lee:** Resources, Data curation. **Jungho Hwang:** Resources, Data curation, Funding acquisition. **Eun-Kyung Lim:** Conceptualization, Methodology, Software, Formal analysis, Investigation, Writing – review & editing, Project administration. All authors have read and agreed to the published version of the manuscript.

Environmental Implication

Airborne pathogens infect many people and pose an increasingly serious threat to public health. In this study, we developed a portable smartphone-based colorimetric sensor to detect and monitor airborne pathogens (e.g., bacteria) *in situ*. This sensor utilizes the CRISPR-Cas12a system to recognize specific DNA sequences in bacteria, enabling visual detection by causing a color change. In addition, developing an analysis application (app) for smartphones makes it possible to check the presence of bacteria regardless of the external environment (brightness, camera specifications). This system enables a preemptive response from airborne infectious diseases.

Declaration of Competing Interest

The authors declare that they have no known competing financial interests or personal relationships that could have appeared to influence the work reported in this paper.

Data Availability

Data will be made available on request.

Acknowledgements

This research was supported by the National Research Foundation (NRF) grants funded by the Korean Government (MSIT; grant numbers: NRF-2021M3E5E3080379, NRF-2021M3H4A1A02051048, NRF-2021M3E5E3080844, and NRF-2022R1C1C1008815), Technology Development Program for Biological Hazards Management in Indoor Air through the Korea Environment Industry & Technology Institute (KEITI) funded by the Korean Government (ME; grant number: 2021003370003), Korea Evaluation Institute of Industrial Technology (KEIT) grant funded by the Korean Government (MOTIE; grant number:

RS-2022-00154853), Nanomedical Devices Development Program of the National Nano Fab Center (grant number: CSM2105M101), and KRIBB Research Initiative Program (grant number: KGM5472322).

Appendix A. Supporting information

Supplementary data associated with this article can be found in the online version at doi:10.1016/j.jhazmat.2023.132398.

References

- [1] Baker, R.E., Mahmud, A.S., Miller, I.F., Rajeev, M., Rasambainarivo, F., Rice, B.L., Takahashi, S., Tatem, A.J., Wagner, C.E., Wang, L.F., Wesolowski, A., Metcalf, C.J. E., 2022. Infectious disease in an era of global change. *Nat Rev Microbiol* 20, 193–205. <https://doi.org/10.1038/s41579-021-00639-z>.
- [2] Boles, M.A., Engel, M., Talapin, D.V., 2016. Self-assembly of colloidal nanocrystals: from intricate structures to functional materials. *Chem Rev* 116, 11220–11289. <https://doi.org/10.1021/acs.chemrev.6b00196>.
- [3] CIE, Cambridge University Press, Cambridge, UK, 1932.
- [4] Davey, H.M., 2011. Life, death, and in-between: meanings and methods in microbiology. *Appl Environ Microbiol* 77, 5571–5576. <https://doi.org/10.1128/AEM.00744-11>.
- [5] Dietrich, R., Jessberger, N., Ehling-Schulz, M., Märklbauer, E., Granum, P.E., 2021. The food poisoning toxins of *Bacillus cereus*. *Toxins* 13, 98–146. <https://doi.org/10.3390/toxins13020098>.
- [6] Fang, Z., Yao, W., Lou, X., Hao, C., Gong, C., Ouyang, Z., 2016. Profile and characteristics of culturable airborne bacteria in Hangzhou, Southeast of China. *Aerosol Air Qual Res* 16, 1690–1700. <https://doi.org/10.4209/aaqr.2014.11.0274>.
- [7] Gao, G., Wang, D., Brocenschi, R., Zhi, J., Mirkin, M.V., 2018. Toward the detection and identification of single bacteria by electrochemical collision technique. *Anal Chem* 90, 12123–12130. <https://doi.org/10.1021/acs.analchem.8b03043>.
- [8] Griffin, D.W., 2007. Atmospheric movement of microorganisms in clouds of desert dust and implications for human health. *Clin Microbiol Rev* 20, 459–477. <https://doi.org/10.1128/CMR.00039-06>.
- [9] Ki, J., Na, H.K., Yoon, S.W., Le, V.P., Lee, T.G., Lim, E.K., 2022. CRISPR/Cas-assisted colorimetric biosensor for point-of-use testing for African swine fever virus. *ACS Sens* 7, 3940–3946. <https://doi.org/10.1021/acssensors.2c02007>.
- [10] Kim, H., Lee, S., Seo, H.W., Kang, B., Moon, J., Lee, K.G., Yong, D., Kang, H., Jung, J., Lim, E.K., Jeong, J., Park, H.G., Ryu, C.M., Kang, T., 2020. Clustered regularly interspaced short palindromic repeats-mediated surface-enhanced Raman scattering assay for multidrug-resistant bacteria. *ACS Nano* 14, 17241–17253. <https://doi.org/10.1021/acsnano.0c07264>.
- [11] Kim, H.R., An, S., Hwang, J., 2021. High air flow-rate electrostatic sampler for the rapid monitoring of airborne coronavirus and influenza viruses. *J Hazard Mater* 412, 125219. <https://doi.org/10.1016/j.jhazmat.2021.125219>.
- [12] Kim, K.H., Hwang, A., Song, Y., Lee, W.S., Moon, J., Jeong, J., Bae, N.H., Jung, Y. M., Jung, J., Ryu, S., Lee, S.J., Choi, B.G., Kang, T., Lee, K.G., 2021. 3D hierarchical nanotopography for on-site rapid capture and sensitive detection of infectious microbial pathogens. *ACS Nano* 15, 4777–4788. <https://doi.org/10.1021/acsnano.0c09411>.
- [13] Kooker, J.M., Fox, K.F., Fox, A., 2012. Characterization of micrococci strains isolated from indoor air. *Mol Cell Probes* 26, 1–5. <https://doi.org/10.1016/j.mcp.2011.09.003>.
- [14] Loesdau, M., Chabrier, S., Gabillon, A., 2014. In: Elmoataz, A., Lezoray, O., Nouboud, F., Mammass, D. (Eds.), *Image and Signal Processing*, Vol. 8509. Springer International Publishing, Cham, pp. 203–212.
- [15] Maier, T., Klepel, S., Renner, U. and Kostrzewa, M., 2006. Fast and reliable MALDI-TOF MS-based microorganism identification. 3, i-ii. <https://doi.org/10.1038/nmeth870>.
- [16] Maldonado-Miranda, J.J., Castillo-Pérez, L.J., Ponce-Hernández, A., Carranza-Álvarez, C., in: Dar, G.H., Bhat, R.A., Qadri, H., Al-Ghamdy, K.M., Hakeem, K.R. (Eds.), *Bacterial Fish Diseases*. Academic Press, Cambridge, 2022, Ch. 19.
- [17] Mauriz, E., 2020. Clinical applications of visual plasmonic colorimetric sensing. *Sens (Basel)* 20, 6214. <https://doi.org/10.3390/s20216214>.
- [18] Moon, J., Kwon, H.J., Yong, D., Lee, I.C., Kim, H., Kang, H., Lim, E.K., Lee, K.S., Jung, J., Park, H.G., Kang, T., 2020. Colorimetric detection of SARS-CoV-2 and drug-resistant pH1N1 using CRISPR/dCas9. *ACS Sens* 5, 4017–4026. <https://doi.org/10.1021/acssensors.0c01929>.
- [19] Nnachi, R.C., Sui, N., Ke, B., Luo, Z., Bhalla, N., He, D., Yang, Z., 2022. Biosensors for rapid detection of bacterial pathogens in water, food and environment. *Environ Int* 166, 107357. <https://doi.org/10.1016/j.envint.2022.107357>.
- [20] Patton, E.W., Tissenbaum, M., Harunani, F., 2019. In: Kong, S.C., Abelson, H. (Eds.), *Computational Thinking Education*. Springer, Singapore: Singapore, pp. 31–49.
- [21] Rodriguez, E.A., Correa, M.M., Ospina, S., Atehortua, S.L., Jimenez, J.N., 2014. Differences in epidemiological and molecular characteristics of nasal colonization with *Staphylococcus aureus* (MSSA-MRSA) in children from a university hospital and day care centers. *PLoS One* 9, e101417–e101429. <https://doi.org/10.1371/journal.pone.0101417>.
- [22] Scott, A.T., Layne, T.R., O'Connell, K.C., Tanner, N.A., Landers, J.P., 2020. Comparative evaluation and quantitative analysis of loop-mediated isothermal

- amplification indicators. *Anal Chem* 92, 13343–13353. <https://doi.org/10.1021/acs.analchem.0c02666>.
- [23] Sivakumar, R., Lee, N.Y., 2022. Recent advances in airborne pathogen detection using optical and electrochemical biosensors. *Anal Chim Acta* 1234, 340297. <https://doi.org/10.1016/j.aca.2022.340297>.
- [24] Son, S.U., Jang, S., Kang, B., Kim, J., Lim, J., Seo, S., Kang, T., Jung, J., Lee, K.S., Kim, H., Lim, E.K., 2021. Colorimetric paper sensor for visual detection of date-rape drug γ -hydroxybutyric acid (GHB). *Sens Actuators B Chem* 347, 130598. <https://doi.org/10.1016/j.snb.2021.130598>.
- [25] Son, S.U., Seo, S.B., Jang, S., Choi, J., Lim, J., Lee, D.K., Kim, H., Seo, S., Kang, T., Jung, J., Lim, E.K., 2019. Naked-eye detection of pandemic influenza a (pH1N1) virus by polydiacetylene (PDA)-based paper sensor as a point-of-care diagnostic platform. *Sens Actuators B* 291, 257–265. <https://doi.org/10.1016/j.snb.2019.04.081>.
- [26] Taylor, S.C., Nadeau, K., Abbasi, M., Lachance, C., Nguyen, M., Fenrich, J., 2019. The ultimate qPCR experiment: producing publication quality, reproducible data the first time. *Trends Biotechnol* 37, 761–774. <https://doi.org/10.1016/j.tibtech.2018.12.002>.
- [27] Tornimbene, B., Eremin, S., Escher, M., Griskeviciene, J., Mangani, S., Pessoa-Silva, C.L., 2018. WHO global antimicrobial resistance surveillance system early implementation 2016–17. *Lancet Infect Dis* 18, 241–242. [https://doi.org/10.1016/S1473-3099\(18\)30060-4](https://doi.org/10.1016/S1473-3099(18)30060-4).
- [28] Vogel, N., Retsch, M., Fustin, C.A., Del Campo, A., Jonas, U., 2015. Advances in colloidal assembly: the design of structure and hierarchy in two and three dimensions. *Chem Rev* 115, 6265–6311. <https://doi.org/10.1021/cr400081d>.
- [29] Wen, J., Zhu, Y., Liu, J., He, D., 2022. Smartphone-based surface plasmon resonance sensing platform for rapid detection of bacteria. *RSC Adv* 12, 13045–13051. <https://doi.org/10.1039/d2ra01788a>.
- [30] Zhang, M., Cui, X., Li, N., 2022. Smartphone-based mobile biosensors for the point-of-care testing of human metabolites. *Mater Today Bio* 14, 100254. <https://doi.org/10.1016/j.mtbio.2022.100254>.